DOI: 10.1002/ejic.201000129

Evolution of Metal Complex-Catalysts by Dynamic Templating with Transition State Analogs

Masaomi Matsumoto,[a] Deven Estes,[a] and Kenneth M. Nicholas*[a]

Keywords: Catalyst evolution / Templating / Transition state analogs / Zinc catalysts / Ester hydrolysis

The elicitation of hydrolytic catalysts from a dynamic library of imine-zinc(II) complexes (and their precursor aldehydes and amines) via templating with *pro*-transition state analogs (*pro*-TSA) is described. *pro*-TSA (2-pyridyl)phosphonate **2** amplifies a benzimidazole-derived complex at the expense of an imidazole analogue; the amplified complex is also more active for the hydrolysis of the pyridyl ester **1a**. Employing *pro*-TSA pyridyl hydrate **3** with libraries of Zn complexes of imines having nucleophilic side chains also perturbs the library in favor of imine-Zn complexes which prove to be the more active hydrolytic agents and catalysts. The catalytic hydrolyses exhibit both saturation kinetics and inhibition by the *pro*-TSA. This process for catalyst evolution is operationally simple, amenable to high throughput screening, potentially applicable to a wide variety of catalytic reactions and thus could offer a practical alternative to catalytic antibodies and imprinted polymers.

Introduction

Catalysis is essential to most useful chemical reactions, enabling the conversion to proceed at a practical rate and often with control of chemo-, regio- and stereoselectivity. Rational catalyst design was stimulated by Pauling's hypothesis that enzymes accelerate reactions by complementary binding (stabilization) of the transition state and by Jencks' proposal that protein catalysts could be produced that are complementary to stable transition state analogs (TSAs).[1] These ideas were later realized in the invention of catalytic antibodies by Schultz and Lerner.[2] More recently, TSA-complementary synthetic catalysts have been produced via polymer imprinting.[3] Although antibody and polymer-imprinted catalysts have been developed for a variety of reactions,[4–6] their typically modest activity,[7,8] limited catalytic functionality, expensive and complex production technology (for antibodies), and structural heterogeneity (for imprinted polymers) have hampered their practical use.

Seeking a new and potentially more useful process for catalyst evolution we turned to dynamic combinatorial chemistry,[9] in which a substrate (or potentially a TSA) is employed to select complementary receptors (or catalysts) that are in equilibrium with a set of chemical building blocks. Generally, free energy minimization favors enhanced production (amplification) of the strongest binding species to the template,[9b] which, if a TSA, should be the best catalyst according to Pauling–Jencks. The ability of such equilibrating systems to amplify receptors has been amply demonstrated, but *catalyst production* via dynamic-TSA association is very rare and has achieved only modest activities.[10] A disulfide cyclic trimer, amplified by cationic TSAs was reported by Sanders and co-workers[10a] to have a twofold rate acceleration for acetal hydrolysis (compared to background) and catalyzed a cationic Diels–Alder addition with a k_{cat} of 1.9×10^{-3} s^{-1}.[10b]

Inclusion of metal complexes into dynamic libraries[11] has great potential for TSA-based catalyst generation given their typical labilities, strong substrate/TSA-binding, and diverse catalytic activities. Morrow and co-workers used dynamic combinatorial chemistry to select chelators for extracting zinc or cadmium into chloroform.[11e] The Lehn[11a] and Nitschke[11d] groups have demonstrated that complex dynamic libraries of ligands can be made to form predominately one discrete product metal complex through self-selection. However, no catalytic metal complexes have been produced from dynamic libraries of metal-ligand complexes.

We envisioned the evolution of hydrolytic catalysts from a library of metal complexes in equilibrium with imine ligands[11] and their precursor building blocks by templating with *pro*-transition state analogs to form ternary complexes, LM(*pro-TSA*) (Figure 1). Considering prior studies of metal ion catalysis of hydrolytic reactions the coordinating metal center would promote hydrolysis by increasing the electrophilicity of the substrate, stabilizing the developing tetrahedral intermediate, and/or increasing the acidity and nucleophilicity of water.[12] With a strongly coordinating substrate, pyridyl-CO_2R, addition of M–OH to the bound

[a] Department of Chemistry and Biochemistry, University of Oklahoma,
Norman, OK 73019, U.S.A
Fax: +1-405-325-6111
E-mail: knicholas@ou.edu

Supporting information for this article is available on the WWW under http://dx.doi.org/10.1002/ejic.201000129.

 © 2010 Wiley-VCH Verlag GmbH & Co. KGaA, Weinheim

substrate is rate-limiting (Figure 2).[13] *pro*-TSAs **2**[14] and **3**[15] were thus selected to simulate the TS of metal-mediated hydrolysis. Here we report the first examples of the elicitation of metal complex catalysts by dynamic templating with transition state analogs.

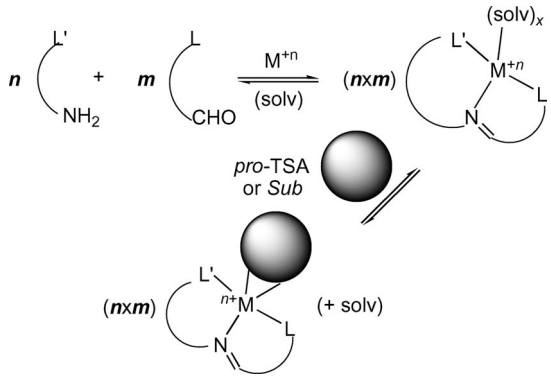

Figure 1. Dynamic templating of imine-Zn complexes.

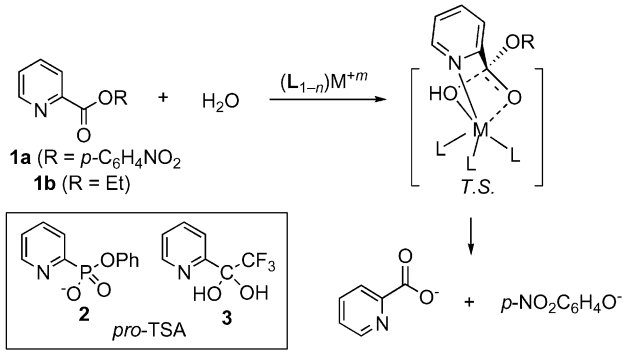

Figure 2. Metal-ion catalyzed hydrolysis of pyridyl carboxyl esters.

Results and Discussion

Zinc-promoted imine exchange was employed to produce sets of equilibrating imine-Zn(solv)$_n^{x+}$ complexes from aldehydes and amines (Figure 3).[16] A 1.0:0.9 mixture of (**4**)- and (**5**)Zn(solv)$_n^{x+}$ was thus produced from the precursor aldehydes, $PyCH_2CH_2NH_2$ and $Zn(OTf)_2$ (1:1:1:1, 50–95% CH_3CN/H_2O, 20 °C, 24 h), established by BH_4^-/HPLC quench/analysis.[17,18] Addition of *pro*-TSA **2** (0.5–2.0 equiv.) to the (L)Zn(solv)$_n^{x+}$ library (20 °C, 24 h) caused the quantity of benzimidazole derivative **5** *to be amplified 1.4-fold* (and **4** attenuated by 0.9, Figure 4). That the amplification is mediated by the formation of ternary (imine)-Zn(*pro*-TSA)$^+$ complexes was shown by Job's plots (see SI) and ESI-MS, which showed major species of composition (**4**)Zn(**2**)$^+$ (*m*/e = 512) and (**5**)Zn(**2**)$^+$ (*m*/e-562). In addition, a competitive ^{31}P NMR titration (monitoring the phosphorus nucleus in *pro*-TSA **2**) and Scatchard analysis[19] between preformed (**4**)Zn(**2**)$^+$ and (**5**)Zn(**2**)$^+$ with the weaker binding substrate analog ethyl picolinate **1b** [Equation (1)] showed the relative affinities of anionic *pro*-TSA **2** vs. neutral **1b** to be 19 for (**5**)Zn(**2**)$^+$ and 10 for (**4**)Zn(**2**)$^+$. These results demonstrate both the greater affinity of LZn^{x+} for the anionic *pro*-TSA over the neutral substrate, which should translate into catalytic activity, as well as the differential binding induced by the auxiliary ligands.

(**4**)Zn(**2**)$^+$ + **1b** ⇌ (**4**)Zn(**1b**)$^+$ + **2** (1)

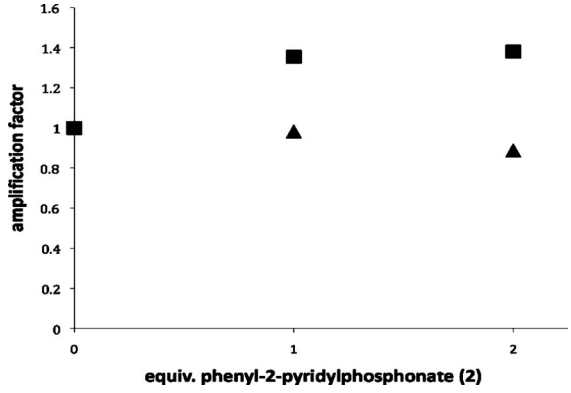

Figure 4. Templating of (**4**,**5**)Zn(solv)$^{x+}$ with *pro*-TSA **2**. black filled squares: reduced **5**; black filled triangles: reduced **4**; amplification factor = $[L_{templated}]/[L_{untemplated}]$.

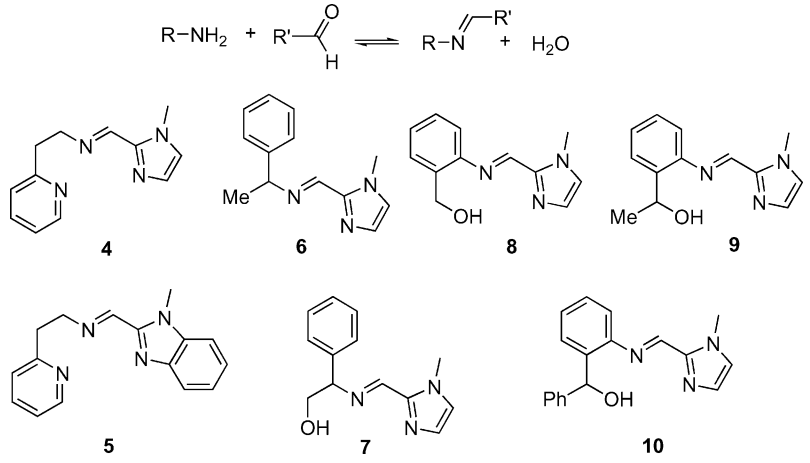

Figure 3. Reversibly formed (dynamic) imine ligands.

 © 2010 Wiley-VCH Verlag GmbH & Co. KGaA, Weinheim

The correlation between *pro*-TSA affinity and hydrolytic reactivity was first assessed by comparing the single-turnover hydrolysis of picolinate **1a** (82 mM) in 30% methanol/MOPS (pH 7.5, 25 °C) promoted by (**4**)Zn(solv)$_n^{x+}$ and (**5**)Zn(solv)$_n^{x+}$ (0.2–0.6 mM), monitored at 400 nm. The second-order rate constants (Table 1, library I) correlate qualitatively with the templating behavior, in favor of the benzimidazole complex, 1.5-fold for *pro*-TSA binding and threefold in rate. Also, *pro*-TSA **2** (0–10 mM) was found to competitively inhibit the (L)Zn-promoted hydrolysis of **1a** approximately twofold. We interpret the ligand-dependent binding and kinetics for the **4/5**-Zn system as being derived primarily from the lower basicity of the benzimidazole ligand **5** (increasing the Lewis acidity of its Zn complex),[20] which should stabilize the ternary zinc complex with anionic **2** and accelerates hydrolysis through transition state stabilization.

Table 1. *pro*-TSA binding, amplification, and hydrolytic rate constants.

LZn(solv)$^{n+}$, L =	TSA	AF[a]	k(M^{-1} min^{-1}), STO[b] (MTO)[c]
Library I			
4	**2**	0.9	30
5	**2**	1.4	90
Library II			
6	**3**	0.5	170
7	**3**	2.0	432
Library III			
7	**3**	0.5	432
8	**3**	2.5	1930
Library IV			
7	**3**	0.8	432 (70)
8	**3**	2.8	1930 (118)
9	**3**	0.9	202 (64)
10	**3**	0.3	234 (45)

[a] AF (amplification factor) = [$L_{templated}/L_{untemplated}$]. [b] Single turnover hydrolysis rate constant for **1a**. [c] Multiple turnover rate constant for hydrolysis of **1a**.

To further illustrate catalyst elicitation by TSA-templating, equilibrating ligands **7**–**10** were produced that could participate in covalent interactions with a *pro*-TSA via nucleophilic side chains, e.g. **3**, and hence in nucleophilic co-catalysis.[21,22] Addition of **3** to the pair (solv)Zn(**6**)$^+$ (lacking an -OH) and -(**7**) caused a 1.7-fold increase of **7** and a decrease of **6** by a half (L-II, Table 1 and SI). In contrast, addition of **3** to (solv)Zn-**7**,**8** (LIII) caused a 2.5-fold increase in **8** and a 0.5-fold decrease of **7**. In both cases ESI-MS spectra revealed major species of composition (**L**)Zn(**3**-H_2O)$^+$, suggesting formation of hemiketal ternary complexes (Figure 5), **11** and **12**. Importantly, *the activity of (**6**)-, (**7**)- and (**8**)Zn(solv)$_n^{x+}$ for **1a** hydrolysis* (25% methanol/MOPS, pH 7.5, 25 °C) varied considerably, again *paralleling the templating trend* (Table 1), i.e. (solv)$_n$Zn-(**8**) > -(**7**) > -(**6**).

Interestingly, exposing these libraries to TSA **2** has the opposite effect; addition of *pro*-TSA **2** elicited a 1.3-fold amplification of **6** and a 0.6-fold attenuation of **7** in the pair (solv)Zn(**6**)$^+$ and -(**7**). Addition of **2** elicited a twofold amplification of **7** and a 0.5-fold attenuation of **8** from the pair (solv)Zn(**7**)$^+$ and (**8**). In both these cases, amplification elicited by **2** does not correlate with catalytic activity. This suggests that the structure of the *pro*-TSA contains information regarding the mechanism of the catalysis. Since catalysis by ligands **7** and **8** most likely go through an intramolecular nucleophilic attack by a hydroxy, only *pro*-TSA **3**, which has the ability to form the hemiketal adduct, is an accurate *pro*-TSA for catalysis by (solv)Zn(**7**)$^+$ and (**8**). *pro*-TSA **2**, which lacks the ability to exchange nucleophilic oxygens under our experimental conditions, is a poor *pro*-TSA for nucleophilic co-catalysis by the ligand. This behavior illustrates the need for careful selection of the *pro*-TSA to mimic the mechanism of the desired reaction.

Investigating a larger library (LIV) of hydroxyimine-Zn complexes from **7**–**10** (Figure 3), addition of *pro*-TSA **3** produced *a nearly threefold amplification of **8***, with attenuation of **7**, **9**, and **10** (Table 1). ^{19}F NMR Job plots and ESI-MS of (**7**–**10**)Zn(solv)$^+$ + **3** show the presence of primarily LZn(**3**)$^+$ and some $L_2Zn_2(3)_2^{2+}$ species (SI). Rate constants for the hydrolysis of **1a** by (**7**)-, (**8**)-, (**9**)- and (**10**)Zn-(solv)$_n^{x+}$ varied almost 10-fold, paralleling the templating

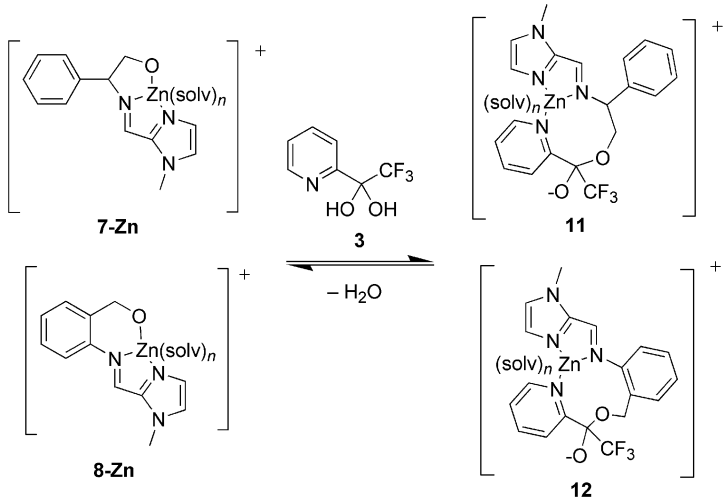

Figure 5. Formation of ternary complexes between (**7**)Zn(solv)$^+$ and (**8**)Zn(solv)$^+$ with *pro*-TSA **3**.

 © 2010 Wiley-VCH Verlag GmbH & Co. KGaA, Weinheim

results. Moreover, *under catalytic conditions* [2.5–10 mol-% LZn(solv)$_n$ vs. **1a**] *the initial rate constants for (solv)Zn(7–10) correlate linearly with the templating behavior* with **3** (R^2 = 0.98, Table 1, Figure 6), again with (**8**)Zn(solv)$_n^{x+}$ being the best catalyst. Saturation kinetic behavior (Figure 7) and competitive inhibition by **3** was observed in the hydrolyses catalyzed by (**7**)Zn(solv)$_n^{x+}$ (k_{cat}/k_{uncat} = 51, K_m = 10 mM) and (**8**)Zn(solv)$_n^{x+}$ (k_{cat}/k_{uncat} = 172, K_m = 2 mM), consistent with reversible substrate binding. The wide range in *pro*-TSA affinities and catalytic activity of the Zn complexes of **7**–**10** likely originate from a combination of the weaker donor character of the aromatic imines **8**–**10** (which could stabilize the ternary complex with **3** and increase reactivity) and a differing involvement of the side chain hydroxy group in the transition state caused by geometrical (**7** vs. **8**–**10**) and steric constraints (**8** vs. **9** vs. **10**).

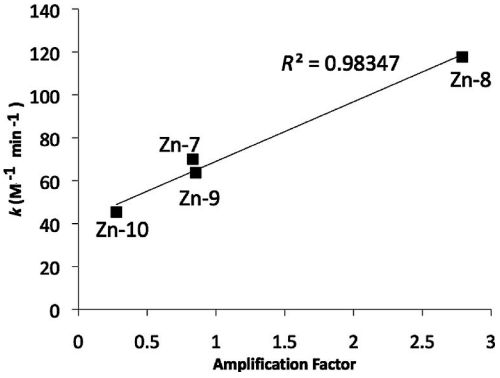

Figure 6. Plot of multiple turnover rate constants vs. amplification factor for *pro*-TSA **3** with **Zn-7**, **Zn-8**, **Zn-9**, and **Zn-10**.

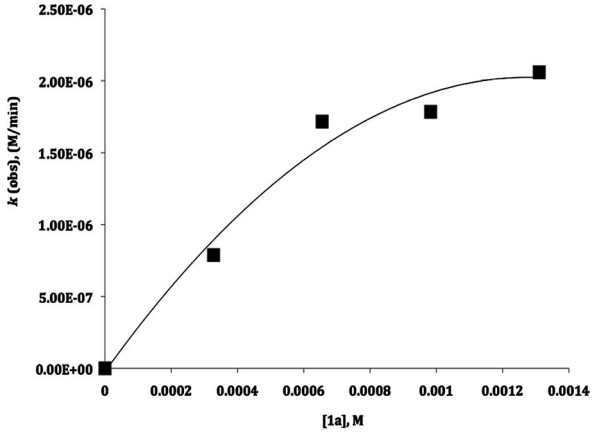

Figure 7. Dependence of the hydrolytic rate constant on the concentration of substrate (4-nitrophenylpicolinate) (**1a**) by the catalyst **7**-Zn(solv).

Conclusions

A set of aldehyde and amine building blocks have been employed to generate equilibrating Zn^{II}-imine complex libraries which respond to templating with *pro*-transition state analogs. The complexes which are thus amplified have proven to be the most active for promoting ester hydrolysis, illustrating the Pauling/Jencks hypotheses for catalyst function and evolution. Our findings thus show that metal complex catalysts can be effectively elicited by dynamic templating with transition state analogs. The process is operationally simple, amenable to high throughput screening, and potentially applicable to a wide variety of catalytic reactions. Further, we have shown that the catalytic mechanism profoundly influences the correct choice of TSA structure. The application of this catalyst evolution process for the enhancement of activity and selectivity for other classes of metal-catalyzed reactions is under investigation.

Experimental Section

General Spectroscopic Methods: ^{1}H, and ^{19}F, and ^{31}P spectra were recorded on a Varian Mercury-300 spectrometer. Mass spectra were acquired on a Finnigan TSQ 700 spectrometer in methanol or acetonitrile solution by ESI. Spectrophotometry was carried out on a Beckman DU 640 spectrophotometer. HPLC analysis was carried out on a Shimadzu Class VP with ZORBAX Eclipse XDB-C18 column (4.6 × 140 mm) at 40 °C.

Materials Preparation: The following were prepared by literature methods: *p*-nitrophenyl picolinate (**1a**),[23] phenyl (2-pyridyl)phosphonate (**2**),[24] 2-pyridyl trifluoromethyl ketone hydrate (**3**),[25] 2-formyl-1-methylbenzimidazole[26] and (*R*,*S*)-1-(2-aminophenyl)ethanol and (*R*,*S*)-(2-aminophenyl)(phenyl)methanol.[27]

Amplification/Analysis Method. General Procedure: A 100 mM stock solution of each building block was produced by dissolving 0.1 mmol of building block in 1 mL of CH_3CN. A 100 mM stock solution of $Zn(OTf)_2$ was prepared in CH_3CN. A 100 mM stock solution of TSA **2** was prepared in 1 mL of CH_3CN and the free base was produced by addition of 14 μL triethylamine. A 100 mM stock solution of TSA **3** was prepared in CH_3CN. Libraries were prepared by pipetting 50 μL aliquots of each building block and $Zn(OTf)_2$ into vials and diluting to 1 mL with CH_3CN. Control libraries contained no TSA, whereas templated libraries were treated with 50–250 μL TSA stock solution **2** or **3**. In cases where the overall solvent composition was to be 50% CH_3CN in water, the samples were diluted to 0.5 mL with CH_3CN and treated with 0.5 mL of water. After equilibrating 24–48 h at 20 °C, the samples were treated with 25 mg of $NaBH_4$ and stirred overnight with a needle in the vial lid to vent excess pressure. Samples were then treated with 100 μL of TFA to acidify, and diluted to 2 mL with water. A 100 μL aliquot of each sample was then taken and diluted to 1 mL in water to provide the HPLC sample.

HPLC Methods: HPLC grade acetonitrile and water with 0.1% v/v TFA were used. Library I, II, and III: 3% acetonitrile 5 min, gradient to 10% acetonitrile over 5 min, 10% acetonitrile 20 min. Library IV: method 1: 5% acetonitrile, gradient to 10% acetonitrile over 5 min, 10% acetonitrile, 20 min. method 2: 15% acetonitrile, 30 min. Library deconvolution was carried out by preparing libraries that were missing one of the building blocks. In cases where there were only three building blocks and two possible Schiff bases, peaks were identified by injecting samples containing building blocks and comparing to chromatograms of libraries containing only one of the possible reduced Schiff bases.

Job's Plot Analysis of Binding Stoichiometry: A 100 mM stock solution of Schiff base-zinc complex was formed in 1 mL of CD_3CN. A 100 mM stock solution of TSA **2** or **3** was prepared in 1 mL of CD_3CN, with 14 μL TEA added in the case of **3**. NMR job plot

 © 2010 Wiley-VCH Verlag GmbH & Co. KGaA, Weinheim

samples were prepared by combining zinc complex and TSA stock solutions in the proportions 10 μL/ 90 μL, 25 μL/75 μL, 50 μL/ 50 μL, 75 μL/25 μL, and 90 μL/10 μL with 900 μL CD_3CN. Samples were analyzed by ^{1}H-NMR and ^{31}P NMR, and ^{1}F-NMR in the case of TSA **3**.

A Job plot for the ternary complex of **5**, zinc(II), and phenyl (2-pyridyl)phosphonate was constructed by observing the ^{31}P NMR chemical shift while simultaneously varying the concentration of Schiff base-zinc complex and phenyl (2-pyridyl)phosphonate. The Job plot shows a local minimum at 1:1 but also a large peak in the high phenyl (2-pyridyl)phosphonate to zinc ratio region, indicating the formation of complexes including multiple phosphonate ligands.

Job plots for the ternary complexes of amino alcohol Schiff bases **7**, **8**, **9**, and **10**, zinc and **3** were constructed by observing ^{19}F NMR chemical shift while varying Schiff base complex and **3**. It was found that the stoichiometry was dependent on the Schiff base. Zinc complexes of **7** and **10** were found to form 2:1 complexes with TSA **3**, of the composition Zn_2**7**$_2$**3** and Zn_2**10**$_2$**3**, whereas zinc complexes of **8** and **9** formed the 1:1 complexes with TSA **3**.

Job plots are provided in the SI.

ESI-MS of Ternary Complexes: ESI-MS of library mixtures for Library I under templating conditions showed the formation of ternary complexes composed of zinc, Schiff base **5**, and phenyl (2-pyridyl)phosphonate, as well as ternary complexes composed of zinc, Schiff base **4**, and phenyl (2-pyridyl)phosphonate.

ESI-MS of the library II mixture shows evidence of the TSA–Schiff base-zinc adduct. Species of interest include a zinc complex of the adduct of **7** and **3**, Zn(**7**)(**3**)(H_2O) (*m*/*z* = 567.07) and a dizinc complex of the composition Zn_2(**7**)$_2$(**3**)(H_2O)$^{2+}$ (*m*/*z* = 379.56).

ESI-MS analysis of the templated library mixture from Library III (Schiff bases **7** and **8**) shows a variety of zinc complexes that incorporate the transition state analog **3**. These include TSA–Schiff base-monozinc complexes Zn(**8**)(**3**)(H_2O) (*m*/*z* = 453.05), Zn(**7**)(**3**)(H_2O) (*m*/*z* = 567.07), and dizinc complexes of the composition Zn_2(**8**)$_2$(**3**)(H_2O)$^{2+}$ (*m*/*z* = 365.54), Zn_2(**7**)(**8**)(**3**)(H_2O)$^{2+}$ (*m*/*z* = 373.56), Zn_2(**7**)$_2$(**3**)(-H_2O)$^{2+}$ (*m*/*z* = 379.56). Also present are peaks corresponding to dizinc complexes without TSA, including Zn_2**8**$_2^{2+}$ (*m*/*z* = 278.06), **Zn$_2$**(**8**)(**7**)$^{2+}$ (*m*/*z* = 285.04), and Zn(**7**)(**2**)$^{2+}$ (*m*/*z* = 292.05).

ESI-mass spectra for these libraries are provided in the SI.

Scatchard Analysis of 4/5 Binding by NMR Titration: A 100 mM solution of Zn (**4**) or Zn (**5**) in CD_3CN was prepared. A 100 mM solution of **2** in CD_3CN was prepared, and 14 μL of triethylamine was added. A 10 mM solution of Zn(**4**)(**2**) or Zn(**5**)(**2**) was prepared from these stock solutions in CD_3CN. Trimethyl phosphate was added as a ^{31}P standard. A 1 M solution of ethyl picolinate in CD_3CN was prepared. Ethyl picolinate **1b** was titrated into the 10 mM solution of Zn(**4**)(**2**) or Zn(**5**)(**2**) in 25 μL aliquots while observing the ^{31}P chemical shift of TSA **2**. A Scatchard treatment of the data gives K_{TSA}/K_{SA} values of 10 for Zn(**4**) and 19 for Zn(**5**)(**2**). The Scatchard graph is provided in the SI.

Single-Turnover Kinetics for the Hydrolysis of 1a Catalyzed by Zn-imine Complexes: Generally, a 4 mM solution of each Zn(ligand) complex was prepared in methanol (25 mL) by combining zinc triflate, aldehyde and amine and allowing the solution to equilibrate 48 h. Analysis by ^{1}H NMR and borohydride reduction/HPLC showed full conversion to the Schiff base. A 0.82 mM solution of **1a** was prepared in 25 mL of CH_3CN. Kinetics runs for Zn(**4**) and Zn(**5**) were made in a 1-cm quartz cuvette containing 1 mL of solution consisting of 700 μL of 100 mM pH 7.5 MOPS buffer, 100 μL of **1a** solution, and Zn(ligand) in methanol varying from 0 to 200 μL with the remaining volume compensated by methanol. The rate of 4-nitrophenyl picolinate hydrolysis by the Schiff base-zinc complexes was measured by spectrophotometric assay at 400 nm. The assay was carried out at 25 °C in the presence of 75% aqueous 100 mM MOPS buffer held at pH 7.5, with catalyst in excess of substrate (single-turnover conditions) over a period of 8 min with one reading per 14 seconds. Plotting (catalyst concentration) × (substrate concentration) vs. the initial hydrolysis rate gives the second-order rate constant. Plots of *k*(obs) vs. Zn complex concentration are provided in the SI.

Inhibition of **1a** hydrolysis by **2** was studied under the same conditions as above while holding catalyst concentration at 0.4 mM and substrate at 82 μM. The concentration of **2** was varied from 0 to 10 mM. **2** appears to inhibit hydroysis by Zn(**4**) and Zn(**5**) with a concentration dependence that levels off rapidly.

Multiple-Turnover Kinetics for the Hydrolysis of 1a Catalyzed by Zn-imine Complexes: The hydrolysis of **1** was carried out under multiple turnover conditions (excess substrate), varying the catalyst concentration. The concentration of **1** was 0.82 mM, and the catalyst concentration was varied from 0.02 mM to 0.08 mM. Reactions were observed for 16 min, with the region from 4–8 min used for the analysis. The assay was carried out at 25 °C in the presence of 75% aqueous 100 mM MOPS buffer held at pH 7.5, and observed at 400 nm. The second-order rate constants for the hydrolysis of 4-nitrophenyl picolinate under multiple-turnover conditions were 70 $M^{-1}min^{-1}$, 117 $M^{-1}min^{-1}$, 63 $M^{-1}min^{-1}$, 45 $M^{-1}min^{-1}$, for Zn-**7**, Zn-**8**, and Zn-**9**, and Zn-**10** respectively. Plots of *k*(obs) vs. [Zn-catalyst][substrate] are provided in the SI.

Saturation Kinetics for Hydrolysis of 1a by Zn(7) and Zn(8): When the 4-nitrophenyl picolinate hydrolysis assay was carried out under conditions of excess substrate (steady state conditions), varying the substrate concentration while holding Zn-Schiff base complex concentration constant, saturation behavior was observed. Kinetics runs for zinc amino alcohol imine ligand complexes were made in a 1-cm quartz cuvette containing 1 mL of solution consisting of 750 μL of 100 mM pH 7.5 MOPS buffer, 250 μL methanol, 40 μM Zn(**7**) or Zn(**8**), and **1a** varying from 0.3 mM to 1.6 mM. Spectrophotometric measurements were made at 400 nm at 25 °C over a period of 8 min with 1 reading per 14 seconds. V_{max} was 5.8×10^{-6} $Mmin^{-1}$ and 2.0×10^{-5} M min^{-1} for Zn-**8** and Zn-**7**, respectively. K_M was 2.0×10^{-3} M and 1.0×10^{-2} M for Zn-**8** and Zn-**7**, respectively. k_{cat} was 0.5 min^{-1} and 0.15 min^{-1} for Zn-**8** and Zn-**7**, respectively. Double reciprocal plots are provided in the SI.

Supporting Information (see also the footnote on the first page of this article): Experimental procedures and data for amplification and kinetics runs, Job's plots, MS data.

Acknowledgments

We thank Prof. Richard Taylor and Prof. Paul Cook for helpful discussions; and Prof. Cook is also thanked for allowing to use his spectrophotometers. M. M. was partially supported by a Graduate Assistantship in Areas of National Need (GAANN) fellowship and D. E. by a D. van der Helm fellowship. We are also grateful for partial support provided by the National Science Foundation (NSF) (CHE-0911158).

[1] L. Pauling, *Am. Sci.* **1948**, *36*, 51.
[2] W. P. Jencks, *Catalysis in Chemistry and Enzymology*, McGraw Hill, **1969**.

 © 2010 Wiley-VCH Verlag GmbH & Co. KGaA, Weinheim

[3] a) A. Tramontano, K. D. Janda, R. A. Lerner, *Science* **1986**, *234*, 1566; b) S. J. Pollack, J. W. Jacobs, P. G. Schultz, *Science* **1986**, *234*, 1570.
[4] G. Wulff, *Chem. Rev.* **2002**, *102*, 1.
[5] a) *Catalytic Antibodies* (Ed.: E. Keinan), John Wiley & Sons, New York, **2005**; b) P. G. Schultz, J. Yin, R. A. Lerner, *Angew. Chem. Int. Ed.* **2002**, *41*, 4427.
[6] a) K. Polborn, K. Severin, *Chem. Commun.* **1999**, 2481; b) K. Polborn, K. Severin, *Chem. Eur. J.* **2000**, *6*, 4604; c) J. J. Becker, M. R. Gagne, *Acc. Chem. Res.* **2004**, *37*, 798.
[7] a) D. Hilvert, chapter 2, in: *Catalytic Antibodies* (Ed.: E. Keinan), **2005**, pp. 30–71, Wiley-VCH, Weinheim, Germany; b) K. N. Houk, A. G. Leach, S. P. Kim, X. N. Zhang, *Angew. Chem. Int. Ed.* **2003**, *42*, 4872.
[8] J.-Q. Liu, G. Wulff, *J. Am. Chem. Soc.* **2008**, *130*, 8044.
[9] a) S. Otto, K. Severin, *Top. Curr. Chem.* **2007**, *277*, 267; b) P. T. Corbett, J. Leclaire, L. Vial, K. R. West, J. L. Wietor, J. K. M. Sanders, S. Otto, *Chem. Rev.* **2006**, *106*, 3652; c) J. M. Lehn, A. V. Eliseev, *Science* **2001**, *291*, 2331; d) J. M. Lehn, *Proc. Natl. Acad. Sci.* **2002**, *99*, 4763.
[10] a) L. Vial, J. K. M. Sanders, S. Otto, *New J. Chem.* **2005**, *29*, 1001; b) B. Brisig, J. K. M. Sanders, S. Otto, *Angew. Chem. Int. Ed.* **2003**, *42*, 1270.
[11] a) C.-F. Chow, S. Fujii, J. M. Lehn, *Angew. Chem. Int. Ed.* **2007**, *46*, 5007; b) J. R. Nitschke, *Acc. Chem. Res.* **2007**, *40*, 103; c) D. M. Epstein, S. Choudhary, M. R. Churchill, K. M. Keil, A. V. Eliseev, J. R. Morrow, *Inorg. Chem.* **2001**, *40*, 1591; d) Z. Grote, R. Scopelliti, K. Severin, *Eur. J. Inorg. Chem.* **2007**, 694; e) S. L. Roberts, R. L. E. Furlan, S. Otto, J. K. M. Sanders, *Org. Biomol. Chem.* **2003**, *1*, 1625.
[12] K. C. Gupta, A. K. Sutar, *Coord. Chem. Rev.* **2008**, *252*, 1420.
[13] a) T. H. Fife, T. J. Przystas, *J. Am. Chem. Soc.* **1985**, *107*, 1041; b) W. L. Mock, H. Cheng, *Biochemistry* **2000**, *39*, 13945.
[14] J. S. Loran, R. A. Naylor, A. Williams, *J. Chem. Soc. Perkin Trans. 2* **1976**, 1444.
[15] R. L. Salvador, M. Saucier, *Tetrahedron* **1971**, *27*, 1221.
[16] C. Godoy-Alcantar, A. K. Yatsimirsky, J. M. Lehn, *J. Phys. Org. Chem.* **2005**, *18*, 979.
[17] ^{1}H-NMR Job plot of **5** vs. $Zn(OTf)_2$ indicates 1:1 stoichiometry. The major species observed in the ESI-MS of **5** + $Zn(OTf)_2$ is $Zn(\mathbf{5})(OTf)^+$; see also Supporting Information).
[18] a) $NaBH_4$ is added to freeze the library composition for HPLC analysis (20 °C, 24 h); b) K. Ziach, J. Jurczak, *Org. Lett.* **2008**, *10*, 5159; c) U. Luning, *J. Incl. Phenom. Macro. Chem.* **2004**, *49*, 81.
[19] L. Fielding, *Tetrahedron* **2000**, *56*, 6151–6170; see also Supporting Information for plot.
[20] M-binding to these ligands parallels pK_a; Me-benzimid (pK_a = 5.6) vs. Me-imid (7.2). G. Jerez, G. Kaufman, M. Prystai, S. Schenkeveld, K. K. Donkor, *J. Sep. Sci.* **2009**, *32*, 1087.
[21] D. S. Sigman, C. T. Jorgensen, *J. Am. Chem. Soc.* **1972**, *94*, 1724.
[22] B. D. Hammock, K. D. Wing, J. Laughlin, V. M. Lovell, T. C. Sparks, *Pesticide Biochem. Physiol.* **1982**, *17*, 76.
[23] D. S. Sigman, C. T. Jorgensen, *J. Am. Chem. Soc.* **1972**, *94*, 1724–1730.
[24] J. S. Loran, R. A. Naylor, A. Williams, *J. Chem. Soc. Perkin Trans. 2* **1976**, 1444–1447.
[25] R. L. Salvador, M. Saucier, *Tetrahedron* **1971**, *27*, 1221–1226.
[26] A. R. Katritzky, H.-Y. He, Q. Long, X. Cui, J. Level, A. L. Wilcox, *ARKIVOC* **2000**, *3*, 240–251.
[27] C. M. Martınez-Viturro, D. Domınguez, *Tetrahedron Lett.* **2007**, *48*, 1023–1026.

Received: February 5, 2010
Published Online: March 13, 2010

 © 2010 Wiley-VCH Verlag GmbH & Co. KGaA, Weinheim